Diagnostic Accuracy of Fused SPECT-CT Images in Comparison with CT, CE-CT, and SPECT for Diagnosis of Pulmonary Thromboembolism

<Original Article>

Diagnostic Accuracy of Fused SPECT-CT Images in Comparison with CT, CE-CT, and SPECT for Diagnosis of Pulmonary Thromboembolism

Fumitoshi AGA[1], Hiroyuki AKAGI[1], Taijyu SHIMBO[1], Tsuyoshi KOMORI[1], Masuo HAYASHI[1], Isamu NARABAYASHI[1], Yoshifumi NARUMI[1] and Takashi YAMADA[2]

1 Department of Radiology, Division of Comprehensive Medicine, Osaka Medical College, Takatsuki-city, Osaka 569-8686, Japan
2 Department of Pathology, Division of Comprehensive Medicine, Osaka Medical College, Takatsuki-city, Osaka 569-8686, Japan

Key words: pulmonary thromboembolism, CT, SPECT, fused image

ABSTRACT

To evaluate the relative accuracy of unenhanced computed tomography (CT), contrast-enhanced CT (CE-CT), single photon emission computed tomography (SPECT), and fused SPECT-CT images for the diagnosis of pulmonary thromboembolism (PTE), 40 cases with suspected PTE were analyzed in a retrospective study. The 40 cases consisted of 22 cases with PTE and 18 cases without PTE. In each case, ^{81m}Kr gas and ^{99m}Tc-macroaggregated albumin SPECT, unenhanced CT and CE-CT were all conducted within a short time span. For this study, the unenhanced CT, CE-CT, SPECT, and fused SPECT-CT images for each case were retrospectively evaluated by receiver operating characteristic (ROC) analysis. ROC analysis showed the Az values for diagnosing PTE were significantly lower in unenhanced CT than in CE-CT, SPECT, or fused SPECT-CT image ($p < 0.05$). Although fused SPECT-CT image showed a higher Az value than either CE-CT or SPECT independent of the radiologists' reading experience, there was no significant difference. These results show that fused SPECT-CT image can be considered a viable alternative diagnostic modality in cases where CE-CT is contraindicated.

INTRODUCTION

Contrast-enhanced computed tomography (CE-CT) is usually the diagnostic modality of choice for diagnosing pulmonary thromboembolism (PTE). CE-CT is contraindicated under certain circumstances, however, such as when patients display an allergic reaction to the contrast media or impaired renal function. In such cases, an alternative methodology is required that provides similar diagnostic accuracy. To determine if fusing unenhanced CT and single photon emission computed tomography (SPECT) images would be useful in assessing PTE, the authors decided to conduct a retrospective

Address correspondence to:
Fumitoshi Aga, Department of Radiology, Division of Comprehensive Medicine, Osaka Medical College, 2-7 Daigaku-machi, Takatsuki-city, Osaka 569-8686, Japan
Phone: +81-72-683-1221(ext.6494) Fax: +81-72-684-6545 E-mail:rad078@poh.osaka-med.ac.jp

study of 40 cases of suspected PTE examined at our hospital.

In PTE, abnormal consolidative opacities due to pulmonary infarction or subsequent atelectasis are occasionally present on CT and mimic those caused by other lung diseases [1-6]. Accurate correlation of these lesions with perfusion defects demonstrated by SPECT in patients with PTE has not yet been well clarified [7, 8].

Recently, Suga et al. developed a method of generating respiratory-gated perfusion SPECT (RGP-SPECT) images [8-10] that facilitates detection of perfusion defects and improves the accuracy of fusion with CT images. Such image fusion can help to clarify the anatomical location of PTE-induced infarction or atelectasis in relation to perfusion defects, and may enhance the differential diagnosis of such lesions from other lung lesions [11].

In this study, the fusion of lung SPECT images with lung CT images was performed using deformable registration. The clinical efficacy of this deformable fusion method in PTE diagnosis was examined by receiver operating characteristic (ROC) analysis, which has been shown to be the only reliable method for visual assessment [12, 13].

SUBJECTS

Among 116 patients who underwent lung ventilation-perfusion scintigraphy for various lung diseases at our institution from November 2006 to May 2008, 40 patients who were suspected of PTE and underwent chest CE-CT imaging within 12 days from SPECT imaging were selected for this study.

In those 40 patients, PTE was identified in 22 patients and not in the rest of 18 patients.

PTE was suspected in patients who presented with dyspnea, low arterial oxyhemoglobin saturation (SaO_2) without improvement following O_2 administration, an increased D-dimer serum level (more than 1.5 μg/ml), and no visible abnormality in the chest X-ray [14].

METHODS

1. Respiratory perfusion SPECT

Lung perfusion SPECT was performed using a two-headed SPECT system (Scanner e.cam duet, Siemens AG, Munich, Germany) with an angular step of 6^{O} and 30 steps, with 10 - 15 sec of acquisition at each step.

^{81m}Kr gas and ^{99m}Tc-macroaggregated albumin (MAA) SPECT as well as a chest CE-CT were acquired within 12 days in each patient. Half of the total ^{99m}Tc-MAA (111 MBq) dose was injected with the patient in a supine position and the remainder in a prone position. SPECT imaging was performed immediately post-injection by the breath step (BrST) method [15]. The BrST method consists of instructing the patient to alternately breathe normally or hold their breath at 10 to 15 sec intervals synchronized with the stepping of the SPECT scanner. ^{81m}Kr gas (185 MBq) was continuously administered during the normal respiration steps. End-inspiratory SPECT images were reconstructed on an image workstation (GMS 5500A/PI, Toshiba Medical Corp., Tokyo, Japan) using a Butterworth low-pass and back-projection filter. A total of 58 to 79 transaxial images over the lungs were reconstructed with a slice thickness of 1 pixel (3.9 mm).

2. CT

CT scanning was performed with a 16-multidetector CT scanner (Aquilion 16, Toshiba Corporation Medical Systems, Tokyo, Japan).

Chest CTs were acquired during deep inspiration breath hold. Scans were obtained at a voltage of 120 or 135 kV, a tube current of real EC (max = 400mAs) (Toshiba Corporation Medical Systems, Tokyo, Japan), 0.5 second per rotation, a detector row beam collimation of 1 mm, and a helical pitch of 15.

The nonionic iodinated contrast agent for the CE-CT images was intravenously administered at a flow rate of 3.0 or 4.0 mL/sec. with a power injector (Dual Shot GX; Nemoto Kyorindo, Tokyo, Japan) through a plastic 20- or 22-gauge intravenous catheter (Terumo, Tokyo, Japan) that was inserted into the cubital vein. The dose of contrast medium was 2 to 2.5 mL per kilogram of weight, and scanning was initiated 20 and 80 or 100 seconds after the start of injection.

The unenhanced CT images were processed at a lung setting (a window width of 1500 and window level of -600), and the CE-CT images were processed at a mediastinal setting (a window width of 300 and window level of 60 or 80).

3. Image registration software

After the images were saved on a picture archiving and communication system (PACS) server, the digital imaging and communication in medicine (DICOM) data were transferred to a PC workstation via the hospital's local area network (LAN), and fused SPECT-CT images were generated using image registration software (LungGuide, Nihon Advanced Biologic Ltd., Osaka, Japan).

For each patient, the LungGuide Derformable

Registration Method (LG-DRM) was applied in four stages. First, a plane of approximate left-right symmetry separating the left lung from the right lung was identified and labeled the midsagittal (MS) plane. MS plane identification was performed independently for the CT and SPECT image data. Second, the optimal rigid registration with six degrees of freedom (3 translational and 3 rotational) between the original lung SPECT and CT images was found by aligning the MS planes and then rigidly translating (shifting) and rotating the SPECT image in 3D so that maximum overlap was achieved between the two images, as measured by a statistical correlation function. Third, the most probable SPECT outer lung surface was estimated and the corresponding anatomic reference points on the CT and SPECT lung surfaces were respectively identified. A one-to-one correspondence between all points on the CT lung surface and all points on the SPECT lung surface was generated, giving a continuous 3D vector displacement field S = S (x,y,z) from one surface to the other. Finally, a scalar deformation energy function E = E (dV) was constructed for a volume displacement field dV = dV (x,y,z) defined on the interior points of the lungs, with the surface mapping S as a boundary constraint. Minimization of the energy function subject to matching point constraints yielded a non-linear mapping of the SPECT volume onto the CT volume, equivalent to a 3D nonlinear fusion of the CT and SPECT images.

4. Image interpretation

The SPECT, unenhanced CT, CE-CT and fused SPECT-CT images were independently reviewed for each patient. Differential diagnosis of PTE was based on the following criteria.

Criteria for unenhanced CT with lung setting:

PTE-induced lesions (infarction/atelectasis) were assumed if the opacity was located in the peripheral area of a segmental or subsegmental wedge-shaped perfusion defect. Consolidative opacities at the peripheral lung interface between severely decreased and relatively preserved perfusion areas were considered to be excellent candidates for PTE [8].

Criteria for CE-CT with mediastinal setting:

A low density area in the main/peripheral pulmonary artery without a significant increase in CT value was considered a strong indication of PTE.

5. Data analysis

ROC curve analysis was performed using a five-grade classification system (1 = normal, 2 = probably normal, 3 = equivocal, 4 = suspicious/probably PTE, 5 = high probability of PTE) to interpret each image. An ROC graph was used for visualizing, organizing, and selecting classifiers on the basis of their diagnostic performance [12, 13]. A diagnosis was made using a simplified two-grade classification system (0 = normal, 1 = PTE).

Three independent radiologists (H.A., T.K. and T.S.), who were blind to the clinical diagnosis, evaluated the images for the presence of PTE. Two of the radiologists (H.A. and T.K.) were nuclear medicine specialists, and the other (T.S.) did not participate in nuclear medicine diagnosis on a routine basis. Differential diagnostic capability was determined by calculating the Az value (Stata 10, StataCorp LP, Texas, USA).

6. Final diagnosis of PTE

1) The primary standard was finding clot formation in the main/peripheral pulmonary artery on the CE-CT images.

2) PTE was also diagnosed on the basis of clinical information, including a low SpO_2 level, increased D-dimer serum level, and improvement on SPECT images following treatment by hemodilution [16, 17]. Such patients were considered to have pulmonary microembolism and diagnosed with PTE despite no visible clot formation in the pulmonary artery on CE-CT.

RESULTS

The ROC curve is shown in Figure 1a-c. For all readers, ROC analysis showed that the Az values in terms of differential diagnosis of pulmonary thromboembolism were significantly lower in unenhanced CT than in CE-CT, SPECT, or fused SPECT-CT image ($p < 0.05$). The Az value of fused SPECT-CT image was generally higher than for SPECT alone or CE-CT, but there was no significant difference. The Az value for fused SPECT-CT image was higher than for CE-CT or SPECT for all three readers despite differing degrees of SPECT reading experience.

Figure 2 is a typical case of acute PTE. CE-CT shows a clot in the pulmonary artery on both sides (Figure 2a). Pulmonary emphysema is seen in S6 of both lungs on unenhanced CT (Figure 2b). Fused SPECT-CT image shows pulmonary infarction in the left S3 and entire right lower lobe as a mismatched area (Figure 2c). Pulmonary emphysema is shown as co-mismatched area in the left S6 on fused SPECT-CT image (Figure 2c).

Figure 3 is a case of chronic PTE. Differential

Figure 1a

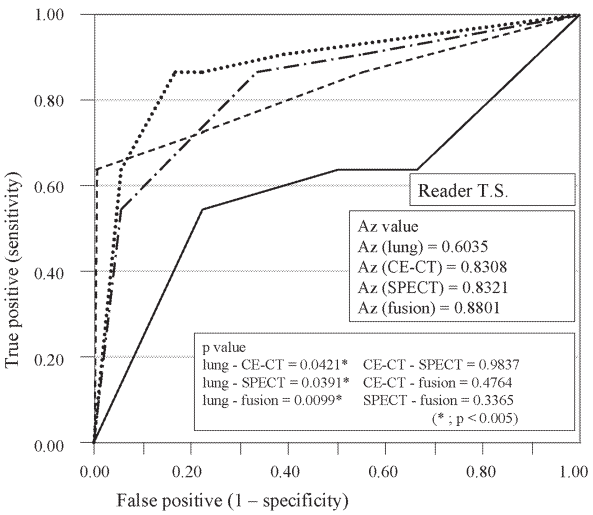

Figure 1b

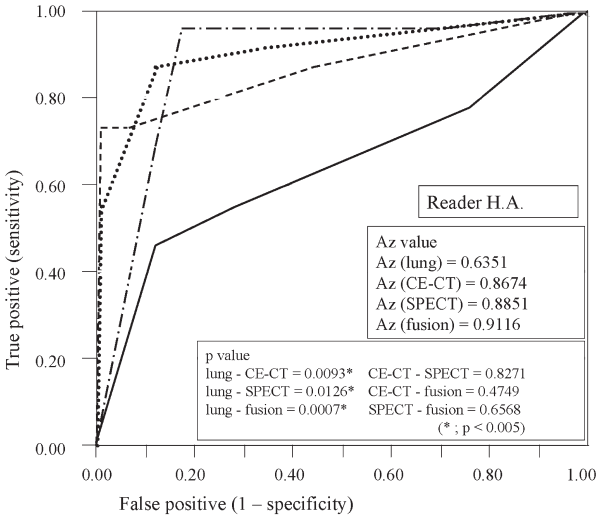

Figure 1c

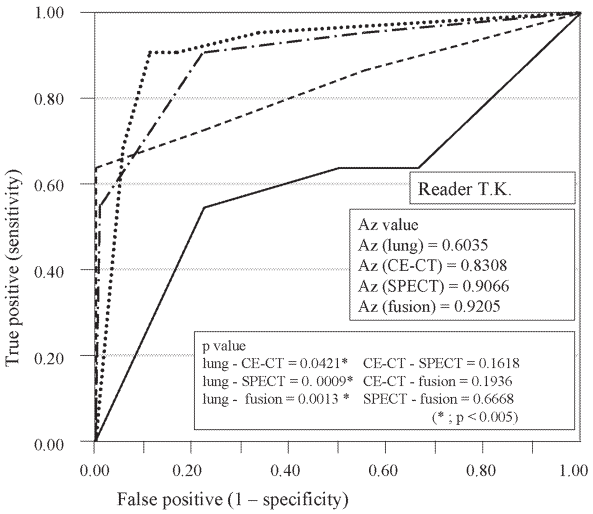

Figure 1 ROC analysis of plain CT, CE-CT, SPECT, and fused SPECT-CT images. For all three readers, the differential diagnostic accuracy (the area under the ROC curve or Az) of the unenhanced CT images was significantly less than for the SPECT, CE-CT, and fused SPECT-CT images ($p < 0.05$). Fused SPECT-CT image showed a higher Az value than either CE-CT or SPECT for all three readers regardless of reading experience.

diagnosis with CE-CT is difficult in the case of chronic and/or miliary PTE if the size of the clot is small. In this case, although the mismatched area is in the right upper lobe on SPECT (**Figure 3a**), no clot formation is visible on CE-CT with a mediastinal setting (**Figure 3b**). Fused SPECT-CT image shows that the mismatched area corresponds to the anatomical right S3 (**Figure 3c**).

Figure 4 is a case of acute pulmonary embolism with abnormal pulmonary findings on unenhanced CT. In addition to a pulmonary arterial thrombus in the right main trunk, dense consolidation is seen in the peripheral lung field (**Figure 4a**), corresponding to the lower perfusion and ventilation area visible on fused SPECT-CT image (**Figure 4b**). It is speculated that the dense consolidation corresponds to the area affected by the pulmonary infarction.

In the SPECT image shown in **Figure 5**, a mismatched area in the entire right lung can be observed, which is consistent with PTE (**Figure 5a**). Although the blood flow in the right S2 was markedly lower, it was difficult to diagnose only by SPECT. However, a more pronounced decrease in blood flow along the consolidation of the lung field was clearly demonstrated by fused SPECT-CT image anatomically.

In **Figure 6** SPECT shows a false positive. CT and SPECT were carried out due to patient dyspnea. Although a small sphenoid mismatched area can be seen in the right dorsal lung field on SPECT

Figure 2a Figure 2b Figure 2c

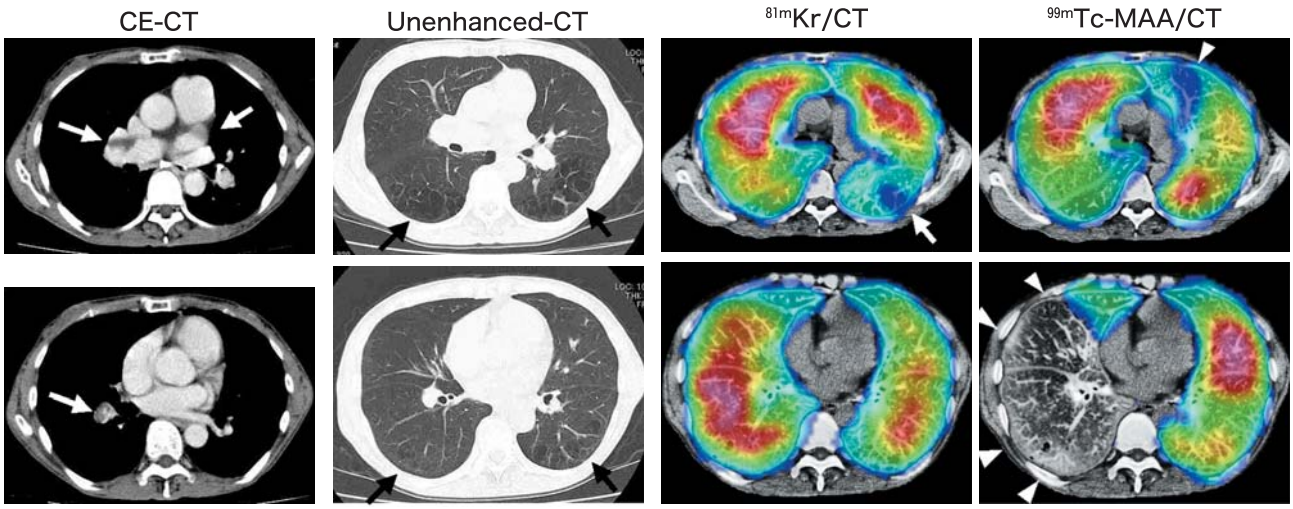

Figure 2 A 62-year-old woman with acute PTE.
a. The CE-CT image shows multiple emboli in the pulmonary artery (white arrows).
b. The unenhanced CT image shows no consolidation in the lung except for lung emphysema, which is seen bilaterally in S6 (black arrows).
c. The fused SPECT-CT image shows mismatched areas in the left S3 and right lower lobe white (arrowheads), and a co-mismatched area in the left S6 (white arrow).

(Figure 6a), clot formation was not demonstrated by CE-CT. Fused SPECT-CT images confirmed that an anatomical fissure line was the cause (Figure 6b).

DISCUSSION

CE-CT is currently indispensable in the diagnosis of PTE [17, 18]. However, in some cases CE-CT is contraindicated due to conditions such as renal insufficiency or a history of previous allergic reaction. In such cases, the physician is faced with diagnosing PTE using only unenhanced CT and SPECT. Fusing the SPECT and unenhanced CT images (SPECT-CT) provides a promising alternative offering greater diagnostic accuracy.

An advantage of fused SPECT-CT image is the capability to obtain anatomical and functional information simultaneously. In SPECT images, demonstration of an area of hypoperfusion and/or hypoventilation can lead to a diagnosis of PTE. However, in some cases anatomical information obtained by lung CT can be very important, as in Figure 6 where a fissure line produces a false positive on SPECT due to perfusion near the pleura being less than further away from the pleura. Another advantage of fused SPECT-CT image is in obtaining detailed location of pathologies such as consolidation or atelectasis that correlate with abnormal areas on SPECT (Figures 2, 4, 5). In case 2, a CT finding of pulmonary emphysema displayed as a co-mismatched area on SPECT, which helped to exclude an additional area of PTE on fused SPECT-CT image. In Figure 5, a subsegmental consolidation near the dorsal pleura was considered to be a PTE-induced infarction due to its preferential location and wedge shape on fused SPECT-CT image.

In this study, ROC analysis showed that diagnostic accuracy using fused SPECT-CT images strongly correlates with diagnosis based on CE-CT. An ROC graph was used for visualizing, organizing and selecting classifiers on the basis of their performance. This method has long been used in signal detection theory to depict the tradeoff between the hit rates and false alarm rates of classifiers [13]. ROC analysis has been improved for use in visualizing and analyzing diagnostic performance [12]. We chose ROC analysis not only because it allowed more objective evaluation in terms of diagnostic performance, but also because it helped us to compare the learning curves of readers with varying clinical experience. In our study, however, there was no statistically significant difference among readers with varying clinical experience in terms of diagnostic performance using CE-CT and fused SPECT-CT image.

Figure 3a

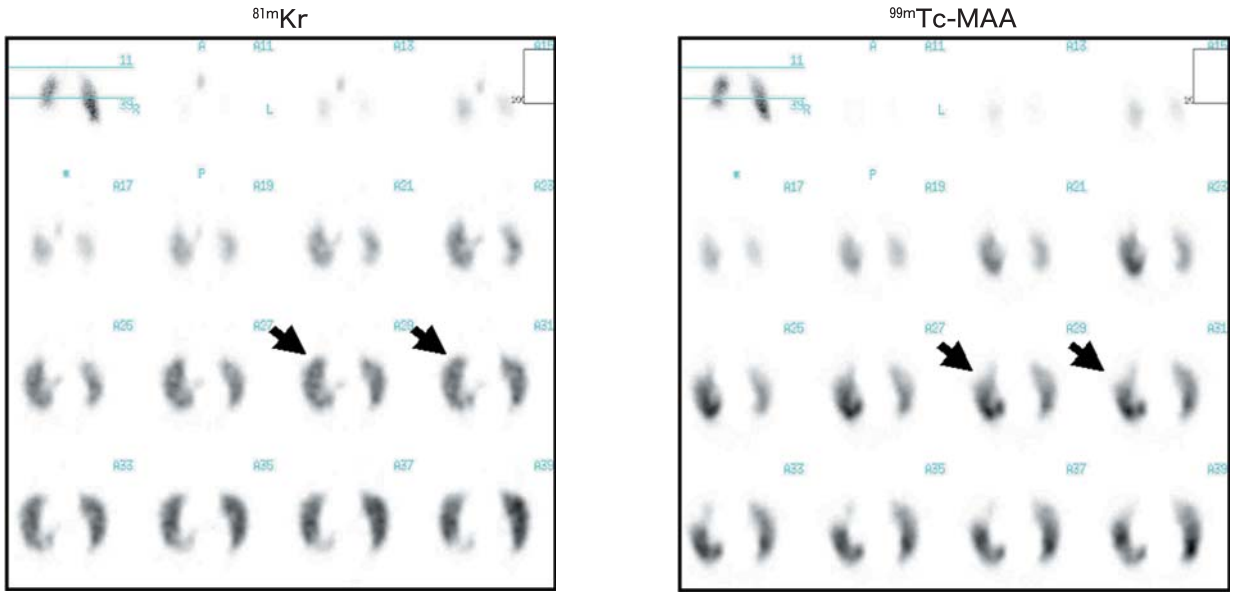

Figure 3b

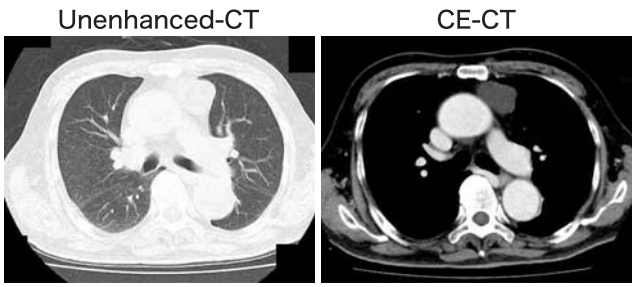

Figure 3c

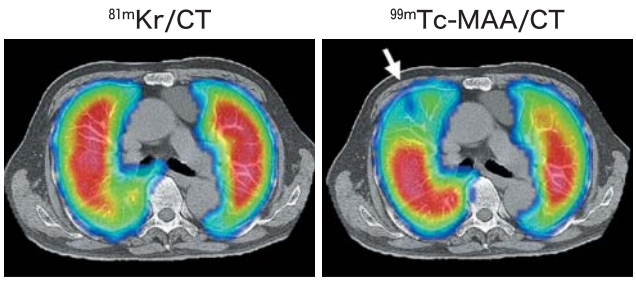

Figure 3 A 74-year-old man with chronic pulmonary micro-thromboembolism.
a. The SPECT image shows a mismatched area in the right S3 (black arrows)
b. The lung field is almost normal on unenhanced CT image with a lung setting as well as CE-CT image with a mediastinal setting.
c. The fused SPECT-CT image shows a mismatched area in the right S3 (white arrow) corresponding to normal lung on the unenhanced CT and CE-CT images.

Figure 4a

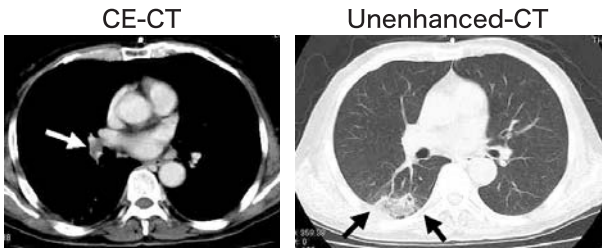

Figure 4b

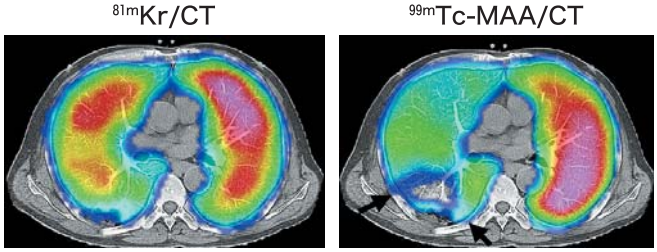

Figure 4 A 68-year-old man with acute PTE.
a. The CE-CT image with a mediastinal setting shows a large clot in the right A6 (white arrow), and unenhanced CT image with a lung setting shows dense consolidation in the peripheral area (black arrows).
b. The fused SPECT-CT image shows excellent matching between the SPECT image defects and consolidation areas (white arrows).

Fig. 5a

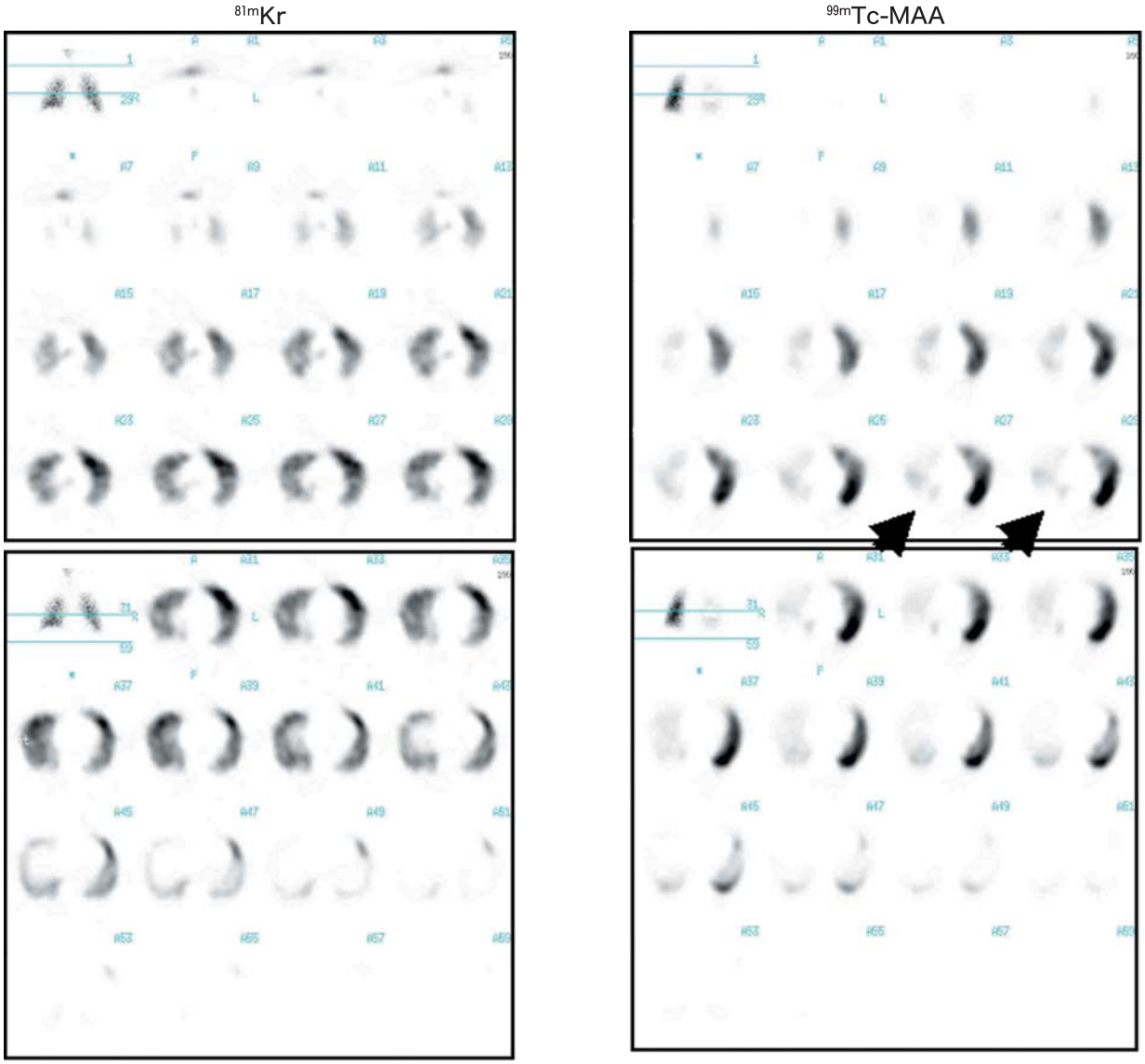

Fig. 5b

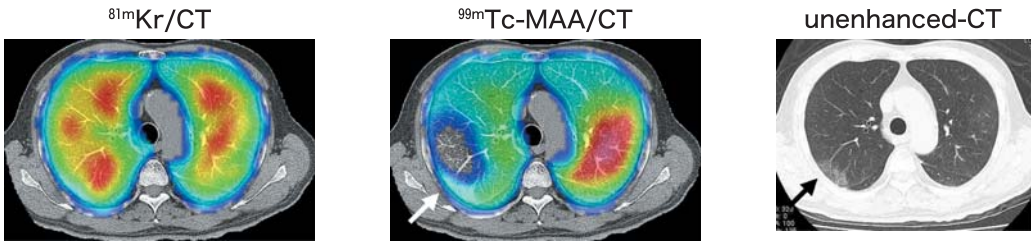

Figure 5 A 77-year-old man with acute PTE.
a. The SPECT images show mismatched areas in the entire right lung, although the blood flow in the right S2 is markedly decreased (black arrows).
b. The fused SPECT-CT image clearly demonstrates that the peripheral subsegmental consolidation on unenhanced CT image (black arrow) corresponds to markedly decreased blood flow along the margin (white arrow).

Figure 6a

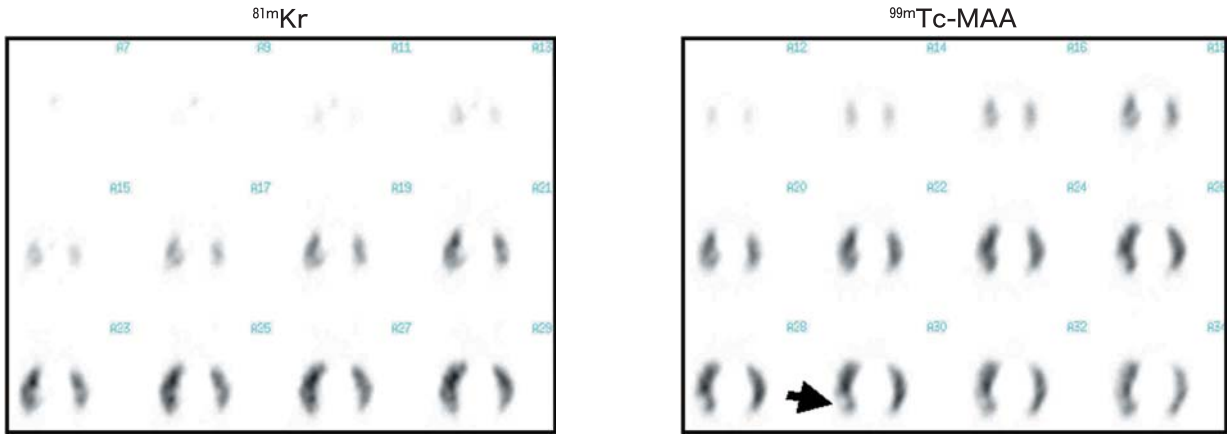

Figure 6b

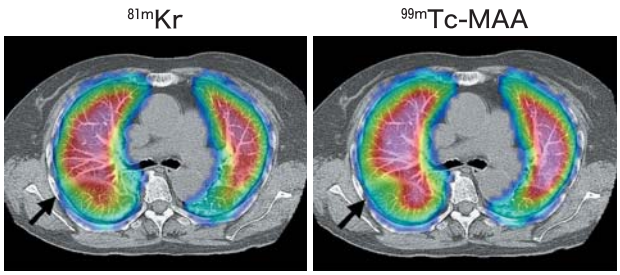

Figure 6 A 74-year-old woman with dyspnea. A false positive with SPECT image and true negative with fused SPECT-CT image.
a. The SPECT image shows a mismatched area in the right middle lower lobe (black arrow).
b. The fused SPECT-CT image shows the mismatched area corresponds to a hypoperfusion area near a fissure line (black arrow).

Among the various modalities used to diagnose PTE, CE-CT has become the mainstay due to the widespread use of multidetector row CT. In this study, as it was difficult to obtain pathological results in our clinical setting, CE-CT plus clinical information was basically considered to be the golden standard in the diagnosis of PTE. However, there were some cases of miliary PTE and chronic PTE in which the SPECT image was essential for accurate diagnosis. In such cases, a final diagnosis of PTE was made based on the SPECT images plus clinical follow-up.

Limitations in our study included a relatively small number of cases and a standard of reference not based on pathological results. Our findings should be further verified by future studies where autopsy or surgical results can be obtained [19, 20].

In spite of these limitations, we believe there is strong evidence to recommend fused SPECT-CT for the diagnosis of PTE when CE-CT is contraindicated. The overlapping of functional and morphological images helps to elucidate associated pulmonary changes and their detailed relationship to blood flow in PTE, enabling accurate diagnosis of PTE independent of a radiologist's reading experience.

ACKNOWLEDGMENTS

The authors wish to thank Peter Fincke, Dr. Hitoya Ohta, Dr. Yasuharu Ogura, Dr. Itaru Adachi, Audrius Stundžia, and Paul Dufort for their excellent technical assistance.

REFERENCES

1. Collart JP, Roelants V, Vanpee D, Lacrosse M, Trigaux JP, Delaunois L, Gillet JB, De Coster P, Vander Borght T. Is a lung perfusion scan obtained by using single photon emission computed tomography able to improve the radionuclide diagnosis of pulmonary embolism? Nucl Med Commun. 2002;23(11):1107-13.
2. Scott AM, Macapinlac HA, Divgi CR, Zhang JJ, Kalaigian H, Pentlow K, Hilton S, Graham MC, Sgouros G, Pelizzari C, et al. Clinical validation

of SPECT and CT/MRI image registration in radiolabeled monoclonal antibody studies of colorectal carcinoma. J Nucl Med. 1994;35(12): 1976-84.
3. Mitomo O, Aoki S, Tsunoda T, Yamaguchi M, Kuwabara H. Quantitative analysis of nonuniform distributions in lung perfusion scintigraphy. J Nucl Med. 1998;39(9):1630-5.
4. Ketai L, Hartshorne M. Potential uses of computed tomography-SPECT and computed tomography-coincidence fusion images of the chest. Clin Nucl Med. 2001;26(5):433-41.
5. Dey D, Slomka PJ, Hahn LJ, Kloiber R. Automatic three-dimensional multimodality registration using radionuclide transmission CT attenuation maps: a phantom study. J Nucl Med. 1999; 40(3):448-55.
6. Kazerooni EA, Whyte RI, Flint A, Martinez FJ. Imaging of emphysema and lung volume reduction surgery. Radiographics. 1997;17(4):1023-36.
7. Howarth DM, Lan L, Thomas PA, Allen LW. 99mTc technegas ventilation and perfusion lung scintigraphy for the diagnosis of pulmonary embolus. J Nucl Med. 1999;40(4):579-84.
8. Zaki M, Suga K, Kawakami Y, Yamashita T, Shimizu K, Seto A, Matsunaga N. Preferential location of acute pulmonary thromboembolism induced consolidative opacities: assessment with respiratory gated perfusion SPECT/CT fusion images. Nucl Med Commun. 2005;26(5):465-74.
9. Suga K, Kawakami Y, Iwanaga H, Tokuda O, Matsunaga N. Automated breath-hold perfusion SPECT/CT fusion images of the lungs. AJR Am J Roentgenol. 2007;189(2):455-63.
10. Suga K, Kawakami Y, Zaki M, Yamashita T, Shimizu K, Matsunaga N. Clinical utility of co-registered respiratory-gated (99m)Tc-Technegas/MAA SPECT/CT images in the assessment of regional lung functional impairment in patients with lung cancer. Eur J Nucl Med Mol Imaging. 2004;31(9):1280-90.
11. Gutman F, Hangard G, Gardin I, Varmenot N, Pattyn J, Clement JF, Dubray B, Vera P. Evaluation of a rigid registration method of lung perfusion SPECT and thoracic CT. AJR Am J Roentgenol. 2005;185(6):1516-24.
12. Hanley JA, McNeil BJ. The meaning and use of the area under a receiver operating characteristic (ROC) curve. Radiology. 1982;143(1):29-36.
13. Swets JA. Measuring the accuracy of diagnostic systems. Science. 1988;240(4857):1285-93.
14. Quinn DA, Fogel RB, Smith CD, Laposata M, Taylor Thompson B, Johnson SM, Waltman AC, Hales CA. D-dimers in the diagnosis of pulmonary embolism. Am J Respir Crit Care Med. 1999;159(5 Pt 1):1445-9.
15. Komori T, Narabayashi I, Hayashi M, Horiuchi S, Adachi I, Ogura Y, Ohta H, Utsunomiya K. Evaluation of breath-hold 201Tl SPECT in the differential diagnosis of solitary pulmonary nodules. Ann Nucl Med. 2005;19(4):277-81.
16. Guidelines on diagnosis and management of acute pulmonary embolism. Task Force on Pulmonary Embolism, European Society of Cardiology. Eur Heart J. 2000;21(16):1301-36.
17. Tapson VF. Acute pulmonary embolism. N Engl J Med. 2008;358(10):1037-52.
18. Tillich M, Schoellnast H. Optimized imaging of pulmonary embolism. Eur Radiol. 2005;15(Suppl 5):E66-70.
19. Kakkar N, Vasishta RK. Pulmonary embolism in medical patients: an autopsy-based study. Clin Appl Thromb Hemost. 2008;14(2):159-67.
20. Steiner I. Pulmonary embolism - temporal changes. Cardiovasc Pathol. 2007;16(4):248-51.

Received November 22, 2008
Accepted January 7, 2009